Microdisk lasers based on GaInNAs(Sb)/GaAs(N) quantum wells

N. V. Kryzhanovskaya ⓘD, E. I. Moiseev, Yu. S. Polubavkina, F. I. Zubov ⓘD, M. V. Maximov, A. A. Lipovskii,
M. M. Kulagina, S. I. Troshkov, V.-M. Korpijärvi, T. Niemi, R. Isoaho, M. Guina, M. V. Lebedev, T. V. Lvova,
and A. E. Zhukov

View Online   Export Citation   CrossMark

ARTICLES YOU MAY BE INTERESTED IN

Lock-in Amplifiers
... and more, from DC to 600 MHz   Watch

Microdisk lasers based on GaInNAs(Sb)/GaAs(N) quantum wells

N. V. Kryzhanovskaya,[1,2,3,a)] E. I. Moiseev,[1] Yu. S. Polubavkina,[1] F. I. Zubov,[1,2]
M. V. Maximov,[1,2,3] A. A. Lipovskii,[1,2] M. M. Kulagina,[3] S. I. Troshkov,[3] V.-M. Korpijärvi,[4]
T. Niemi,[4] R. Isoaho,[4] M. Guina,[4] M. V. Lebedev,[3] T. V. Lvova,[3] and A. E. Zhukov[1,2]

[1]*Nanophotonics Lab, Saint Petersburg National Research Academic University of RAS,
194021 St. Petersburg, Russia*
[2]*Peter the Great St Petersburg Polytechnic University, 195251 St. Petersburg, Russia*
[3]*A. F. Ioffe Physical-Technical Institute of RAS, 194021 St. Petersburg, Russia*
[4]*Optoelectronics Research Centre, Tampere University of Technology, 33720 Tampere, Finland*

We report on microdisk lasers based on GaInNAs(Sb)/GaAs(N) quantum well active region. Their characteristics were studied under electrical and optical pumping. Small-sized microdisks (minimal diameter 2.3 μm) with unprotected sidewalls show lasing only at temperatures below 220 K. Sulfide passivation followed by SiN$_x$ encapsulation allowed us achieving room temperature lasing at 1270 nm in 3 μm GaInNAs/GaAs microdisk and at 1550 nm in 2.3 μm GaInNAsSb/GaAsN microdisk under optical pumping. Injection microdisk with a diameter of 31 μm based on three GaInNAs/GaAs quantum wells and fabricated without passivation show lasing up to 170 K with a characteristic temperature of T$_0$ = 60 K. *Published by AIP Publishing.* [http://dx.doi.org/10.1063/1.4971977]

I. INTRODUCTION

Semiconductors microdisk and microring lasers have been widely investigated as possible building blocks for photonic integrated circuits.[1] The circular symmetry of the cavity results in unique advantages such as low threshold, small foot-print, small mode volume, in-plane emission, control of emission wavelength by the device size, and so on.[2] The use of quantum dots (QDs) as active region in such lasers provides long wavelength emission suitable for avoiding absorption in Si (around 1.3 μm in case of InAs/InGaAs QDs and 1.5 μm in case of InAs/InP QDs) low threshold, and record-high operation temperature (100 °C).[3] However, since the ground state QD optical gain is limited due to the finite number of the QDs,[4,5] the decrease in the resonator diameter to a certain value results in lasing via excited states of QDs.[6] Quantum well (QW) is capable of providing higher maximal gain compared to QDs. Thus, the use of QW active region may help to work out the problem of gain saturation when the laser's size is scaled down. For example, electrically pumped GaInAsP-InP lasers with 2.7 μm diameter and a lasing wavelength ∼1.56 μm operating at 287 K have been demonstrated long ago.[7] Since then the highest operating temperature demonstrated for InP-based microdisk lasers was 50 °C in 50 μm in diameter microring laser.[8] A further increase in the operating temperature of InP-based microlasers is limited by the low confinement energy of the carriers in the active region (small conduction band offsets).

An attractive approach to achieve long wavelength laser emission ($\lambda > 1200$ nm) at high temperatures is the use of GaInNAs(Sb) QWs on GaAs substrates.[9] The material gain of the GaInNAs QW laser is measured as approximately 1200–1300 cm^{-1}.[10] The continuous-wave (CW) operation up to the 100 °C has been demonstrated for 1.3 μm single QW

In$_{0.4}$Ga$_{0.6}$As$_{0.995}$N$_{0.005}$ edge-emitting lasers.[11] High-power semiconductor mm-size disk lasers operating at 1220 nm based on GaInNAs QW have been demonstrated.[12] Then, by adding Sb to GaInNAs alloy, 1.55 μm telecommunication wavelength was reached for both edge emitting lasers[13] and more recently for optically pumped disk lasers.[14] Due to the reactive surfactant properties of antimony, it reduces the group III adatoms surface diffusion length suppressing phase segregation and roughening and thereby improving homogeneity of the alloy.[15,16] Although the growth of quaternary and quinary nitrogen-containing alloys is complex, this approach has been advanced to a level enabling the demonstration of practical devices.[9] In general, compared to InP approach, GaAs-based technology is actually very promising owing to better thermal conductivity, more choices for designing waveguides using AlGaAs/GaAs heterostructures, and somewhat more precise etching and oxidation procedures for nano-structuring. The disadvantage of the GaAs-based material system is one order of magnitude higher surface recombination rate, as compared to InP-based system. In the case of microdisk lasers, this problem can be relieved either by using QDs[17] or by applying surface passivation.[18]

In this paper, we have studied for the first time microdisk lasers based on GaInNAs(Sb)/GaAs(N) QWs operating at both 1.3 μm and 1.5 μm wavelength regions and demonstrate continuous wave (CW) lasing up to 170 K in electrically pumped unpassivated laser and at room temperature in optically pumped sulfide-passivated microlasers.

II. EXPERIMENT

The epitaxial structures were grown by molecular beam epitaxy on n-doped GaAs (100) substrates. Schematic illustration of the layers' sequence in structures containing GaInNAs/GaAs QWs designed for photopumped microdisk lasers (structure A) and for current injection (structure B) are

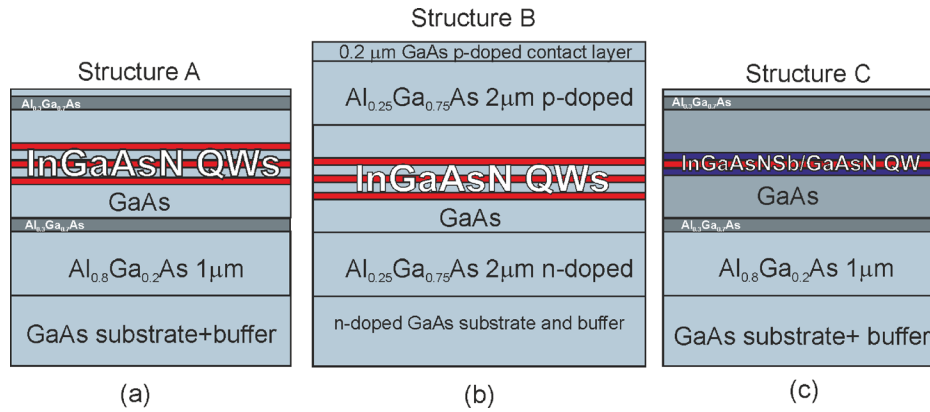a)Author to whom correspondence should be addressed. Electronic mail: NataliaKryzh@gmail.com.

FIG. 1. Schematic illustration of the layers sequence: (a) 1.2 μm GaInNAs/GaAs triple QWs designed for photo-pumped microdisk lasers (structure A); (b) the same triple QWs designed for current injection (structure B); and (c) 1.55 μm GaInNAs(Sb)/GaAsN single QW designed for photopumped micro-disk lasers (structure C).

shown at Figs. 1(a) and 1(b). Three $Ga_{0.7}In_{0.3}N_{0.02}As_{0.98}$ QWs were separated with 10-nm-thick GaAs layers and have ground-state emission peak around 1.2 μm at room temperature. The schematic illustration of the structure with 1.55 μm single $Ga_{0.66}In_{0.34}N_{0.047}AsSb/GaN_{0.029}As$ QW (structure C) is shown at Fig. 1(c). In photopumped structures (A and C), the active region was placed in the middle of the GaAs layer confined from both sides with 10 nm thick $Al_{0.3}Ga_{0.7}As$ barriers to prevent carrier leakage. The total thickness of the waveguide layer in both structures was ~240 nm. This waveguide layer was grown on top of the 1 μm thick $Al_{0.8}Ga_{0.2}As$ layer that later formed a pedestal of the microdisks. The single GaInNAsSb QW was surrounded by 21 nm-thick GaAsN strain-compensating layers. Microdisks of different diameters from 2 to 6 μm were fabricated using photolithography and two step wet etching. A circular mesa was formed by etching in $HBr:K_2Cr_2O_7:CH_3COOH$ solution. The pedestal was formed using diluted HF. Exemplary scanning electron micrograph of a 4 μm diameter photopumped microdisk laser is shown in Fig. 2(a).

In the current-injection structure B, three GaInNAs/GaAs QWs were deposited in the middle of a 0.4 μm thick GaAs waveguide layer confined from both sides with 2 μm thick $Al_{0.25}Ga_{0.75}As$ claddings. The microdisk resonator was formed by means of photolithography and chemical plasma etching to have a diameter of 31 μm. The etching depth was about 4 μm. AgMn/NiAu (AuGe/Ni/Au) metallization was used to form ohmic contacts to p+ GaAs cap layer (n+ substrate, respectively).

For optical investigations, we used a CW YAG:Nd laser ($\lambda = 532$ nm). A piezoelectrically adjustable Olympus LMPlan IR objective $\times 10$ was utilized to focus the incident laser beam to pump the resonator homogeneously as well as to collect the microphotoluminescence (μPL) signal. The μPL was then dispersed via a 1000-mm monochromator Horiba FHR and measured by a cooled InGaAs single-channel detector. The overall spectral resolution was 0.03 nm for 900 l/mm grating. For testing the lasers under current injection, the microlaser chips were mounted epi-side up on a copper heatsink and wired with indium solder, as shown in Fig. 2(b). In-plane emitted light was collected with a piezoelectrically adjustable $\times 50$ Mitutoyo objective and analyzed at the same setup that was used for μPL measurements. For low temperature measurements, the samples were mounted in a flow cryostat Janis ST-500.

III. RESULTS AND DISSCUSSION

A. Characteristics of optically pumped GaInNAs(Sb)/GaAsN microdisk lasers before and after passivation

Optical properties of the GaInNAs(Sb)/GaAs(N) QW media were first investigated using an unprocessed (as-grown) samples A and C in the temperature range of 78–298 K under excitation density of 200 mW/cm². We observe a moderate decrease (by ~8 times) in GaInNAs/GaAs QWs integrated photoluminescence intensity as temperature increases in this temperature interval evidencing high optical quality of the GaInNAs/GaAs QWs (Fig. 3(a)). At low temperature (78 K), full-width at half maximum (FWHM) of the spectrum is ~18 meV, revealing reasonable homogeneity of the GaInNAs/GaAs QW thickness and composition. FWHM monotonically increases to 30 meV with the temperature at 300 K. The wavelength of the GaInNAsSb/GaAsN QW PL spectra maximum is 1.52 μm at room temperature (Fig. 3(b)). The increase in the temperature from 78 K to 298 K results in integral intensity drop by 15 times revealing low non-radiative recombination rate in the 1.55 μm epitaxial structure; FWHM changes from 25 meV to 40 meV.

Emission spectra for the GaInNAs/GaAs QWs microdisks of different diameter (3–6 μm) taken at 78 K are single-mode as shown in Fig. 4(a). A single narrow line corresponding to one of the whispering gallery modes of the resonator is observed on the long-wavelength side of the GaInNAs QW spectra for all the lasers. The output intensity versus input optical pumping power (L-L curves) for the lasing mode is shown in Fig. 4(b) in a log-log scale. Each curve has
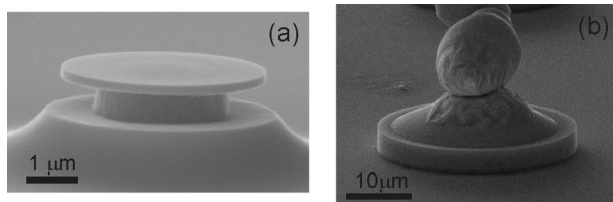

FIG. 2. SEM images of 4 μm diameter photopumped (a) and wired 31 μm injection (b) microdisk lasers with GaInNAs/GaAs quantum wells active region.
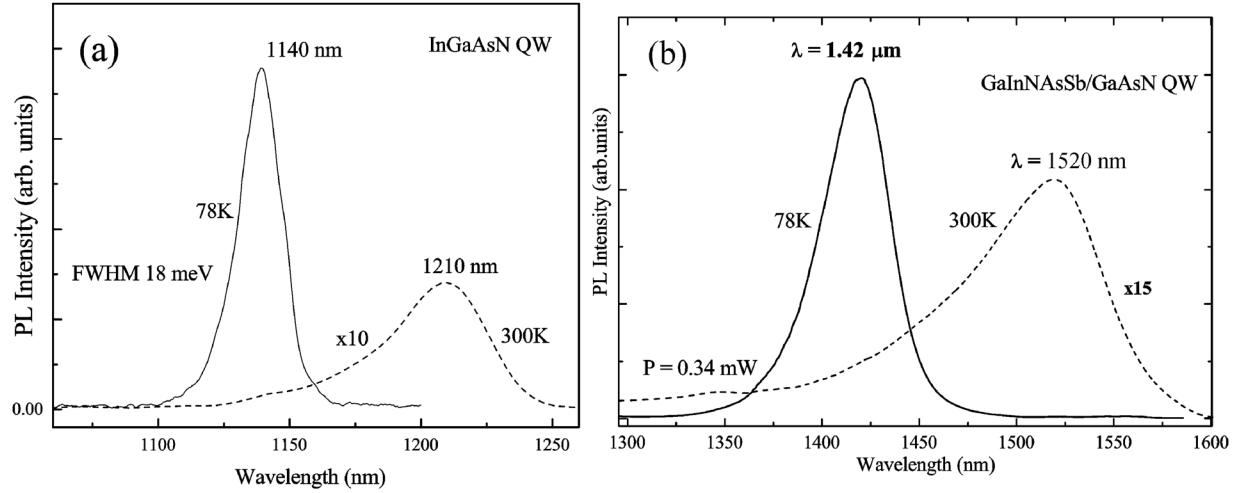
FIG. 3. Photoluminescence spectra of the unprocessed GaInNAs/GaAs QWs (a) and of a single GaInNAsSb/GaAsN QW (b) obtained at 78 K and 300 K.

a pronounced kink, indicating the lasing threshold of the microdisk (marked by arrows). The smallest threshold pump power at 78 K is 0.17 mW for the microlaser with a diameter of 3 μm.

We also fabricated and studied microdiscs (3.7–7.7 μm in diameter) based on single GaInNAsSb/GaAsN QW. Fig. 5 shows μPL spectra of a microdisk laser with diameter $D = 3.7\,\mu$m obtained at different temperatures (at optical pump power P$\sim$1.5P$_{th}$). The spectral position of narrow whispering-gallery mode (WGM) line in the single GaInNAsSb/GaAsN QW μPL spectrum is close to wavelength of spontaneous emission maximum. The inset in Fig. 5(a) shows the dependence of the integrated emission intensities of the lasing WGM line at 78 K on the optical pump power for microdisks of different diameters. From the FWHM of the lasing WGM line just before the threshold (e.g., 0.1 mW for 3.7 μm GaInNAsSb/GaAsN QW microdisk), which is $\sim$50 pm, we estimated the quality factor of the resonator (obtained from $\lambda/\Delta\lambda$) as $\sim$28 000. Threshold pump power vs diameter D of the microlasers dependence is demonstrated in Fig. 5(b). The obtained

thresholds values for GaInNAsSb/GaAsN QW are smaller by 30% than that for microdisks based on GaInNAs QW active region that can be explained by smaller density of states in a single QW active region compared to triple QWs structures. The threshold pump power increases with the enlargement of the resonator area but not proportionally to the squared diameter as could be expected. We attribute this behavior to the increased proportion of the nonradiative recombination at the resonator sidewalls when its diameter decreases. Using the relation between the optical loss and its quality factor, Q$\sim$2πn/($\lambda\alpha$), we can estimate the value of α. In the case of 3.7 μm GaInNAsSb/GaAsN QW microdisk, the Q-factor is $\sim$2.8 $\times$ 10^4, which corresponds to α of about 5 cm^{-1}. This loss can be easily balanced by gain of a single QW. In the case of ultra-small microdisks (with diameter less than 2 μm), surface scattering and radiation leakage may significantly deteriorate the Q-factor and the required gain increases (e.g., Q-factor of 3 $\times$ 10^3 will require an active region with the gain above 50 cm^{-1}). In view of this fact, we used three InGaAsN QWs in structures A and B, where multiple stacking can be done without
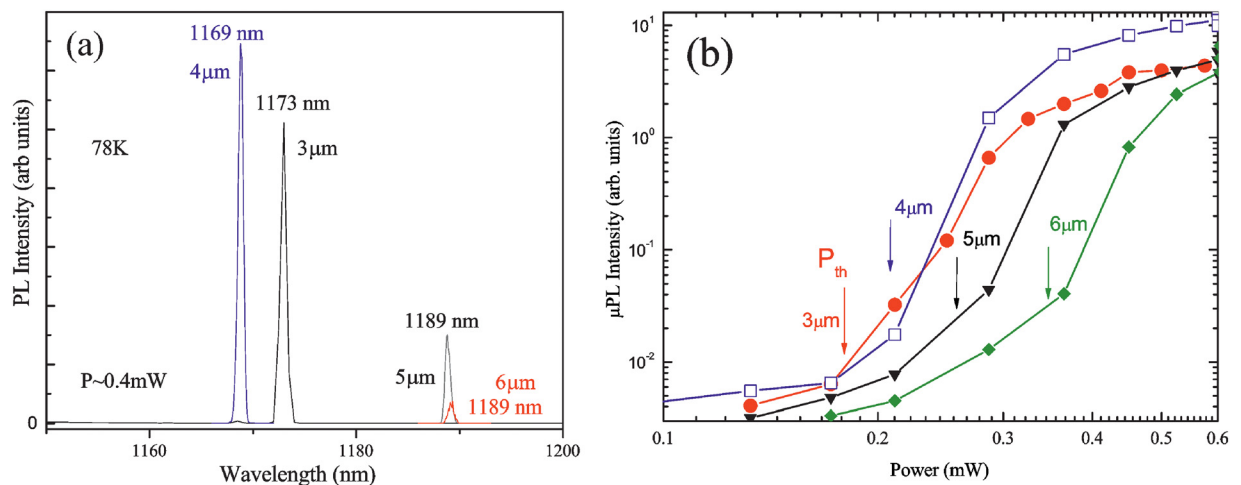

FIG. 4. μPL spectra of the microdisks based on GaInNAs/GaAs QWs obtained at 78 K with 3, 4, 5, and 6 μm cavity diameters (a) and plot of the WGM mode intensity against excitation power for the on GaInNAs/GaAs QW microdisks of 3–6 μm cavity diameters (b).
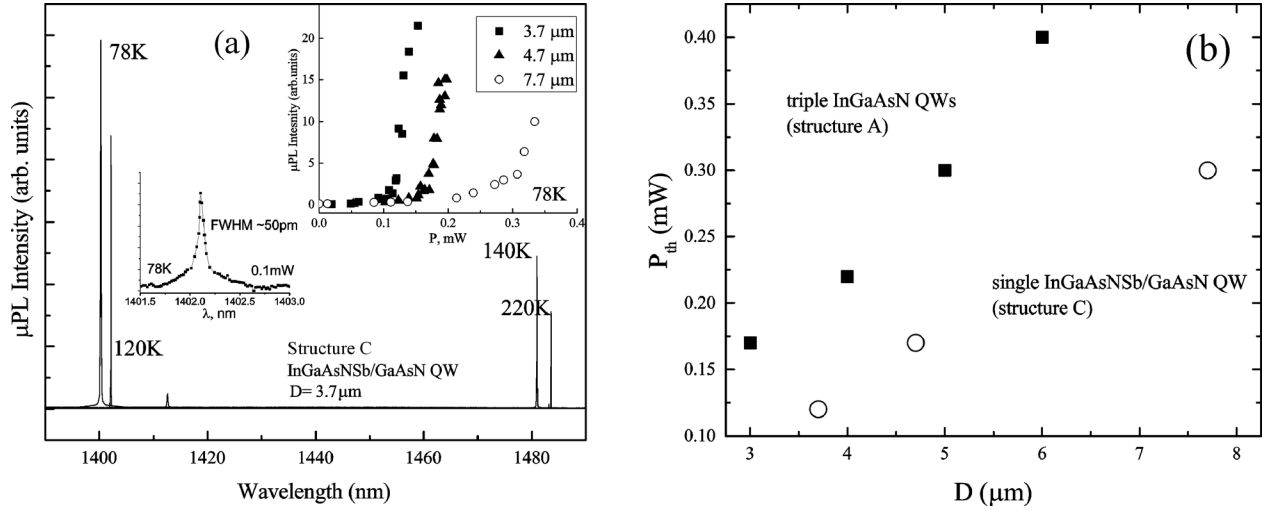
FIG. 5. μPL spectra of the 3.7 μm GaInNAsSb/GaAsN QW microdisk laser obtained at different temperatures (a). Inset: Spectrally integrated emission intensity of WGMs as a function of incident optical pump power for microdisk lasers of different diameters. The threshold pump power at 78 K against the microdisk diameter (b).

degradation of the material quality due to an additionally induced strain. In the case of InGaAsNSb QWs, multiple stacking is challenging because of high strain accumulated.

For all microdisks studied, the emission is TE-polarized and has a narrow far-field diagram in the vertical direction. The lasing in 3 μm in diameter GaInNAs/GaAs QW photo-pumped microdisk was observed up to 130 K. The threshold power increases from 0.17 mW to 0.3 mW in the 78–130 K temperature interval. In 3.7 μm diameter GaInNAsSb/GaAsN QW microdisk, the lasing was observed up to 220 K (Fig. 5(a)), which we attribute to higher carrier confinement energy and slightly larger diameter. When the temperature increases, the spectral position of the resonant line shifts according to temperature induced refractive index change ($\sim$0.06 nm/K). The InGaAsNSb band gap shrinkage is much faster ($\sim$0.47 nm/K). This situation leads to a variation of detuning between the spectral positions of lasing WGM and active media gain maximum with temperature increase, as can be seen from Fig. 6. When the detuning exceeds a certain value, the lasing starts via another mode. Due to this effect, the
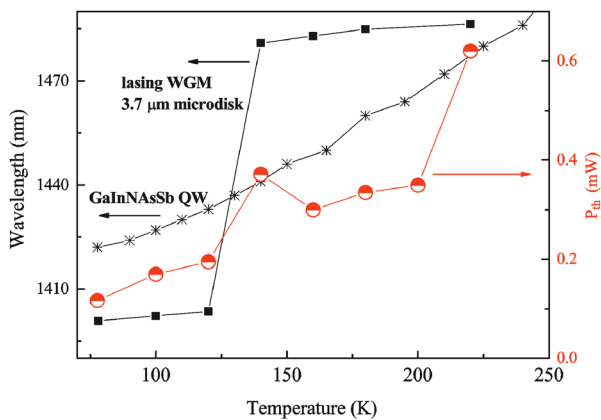

FIG. 6. The spectral position of the lasing WGM line of GaInNAsSb/GaAsN 3.7 μm microdisk laser, the position of the InGaAsNSb QW PL maxima (left axis), and the threshold power of the WGM (right axis) as a function of temperature.

threshold power and lasing wavelength increase step-like near 150 K temperature. At a low temperature (78 K), the threshold power is approximately 0.1 mW and it becomes more than 0.6 mW when the sample temperature grows to 220 K.

To suppress surface non-radiative recombination at microdisk sidewalls that limits high temperature performance, the microdisks fabricated from structures A and C were passivated. The passivation was performed with 1 M aqueous solution of sodium sulphide (Na$_2$S:9H$_2$O) during 4 min, and then, the mesas were washed in water and dried in air. To achieve a good stability of the operation after treatment in sulfur solution, the microdisks were encapsulated by thin (the thickness was approximately 30 nm) SiN layer deposited by PECVD. As a result, the emission was stable over a long time and the experimental results were reproduced after several months. We have not yet succeeded in the development of the passivation treatment for the laser with electrical injection to achieve room temperature operation. The room temperature μPL spectra of the passivated 2.3 μm GaInNAsSb/GaAsN QW microdisks and 3 μm GaInNAs/GaAs QW microdisks at different pump powers are shown in Figs. 7(a) and 7(b). GaInNAsSb/GaAs QW microdisk demonstrates WGM lasing at 1.55 μm with the threshold pump power $\sim$0.5 mW. The wavelength of the lasing WGM line of GaInNAs/GaAs QW microdisk is 1.27 μm with the threshold pump power $\sim$0.8 mW.

A representative room-temperature input-output characteristic of 3 μm GaInNAs/GaAs QW microdisk WGM is shown in inset in Fig. 7(b) in a log-log scale. The β-factor (the fraction of spontaneous emission) for the lasing mode was estimated by fitting the input-output characteristics.[19] We used a rate equation model presented in Ref. 20. The model describes the dependence of the mean photon number in the cavity (n) on the pumping rate (p)

$$p = \frac{\Gamma_c}{\beta}\left[1 + 2\xi + 2\beta(n - \xi)\right]\frac{n}{1 + 2n}, \tag{1}$$
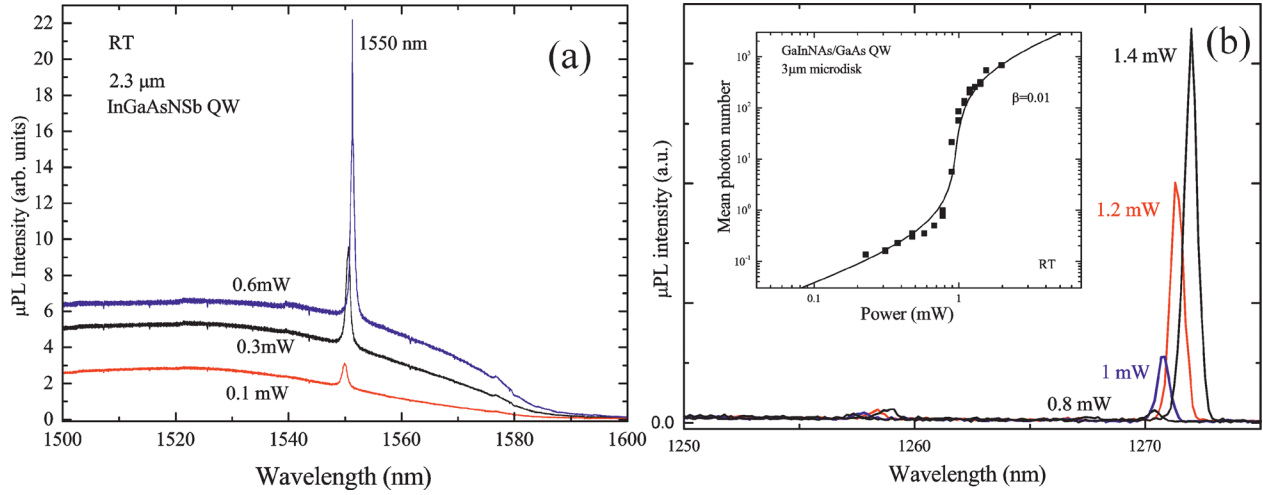
FIG. 7. The μPL spectra of the GaInNAsSb/GaAsN QW microdisk lasers (a) and GaInNAs/GaAs QW microdisk lasers (b) after passivation at 300 K at different pump power. Inset: input-output characteristic of 3 μm GaInNAs/GaAs QW microdisk WGM (dots) and fit based on Eq. (1) (solid).

where Γ is the photon escape rate and ξ is the mean photon number at transparency. A curve of the best fit shown as inset in Fig. 7(b) corresponds to $\beta = 0.015$, $\xi = 0.35$ and $\Gamma = 4 \times 10^{10}\,\mathrm{s}^{-1}$. Previously published values of the β ranges from 0.03 to 0.09.[2,20,21] It should be noted that in our case, residual nonradiative recombination at side walls, even after passivation, can modify the input-output characteristic and thus affect the obtained β-factor value.

B. Characteristics of electrically pumped InGaAsN/GaAs microdisk lasers

We also studied GaInNAs/GaAs injection microdisk lasers with 31 μm diameter. Injection microdisks demonstrate well pronounced turn-on behavior of the current-voltage dependence (the inset in Fig. 8) with 1.4 V turn-on voltage and room-temperature specific series resistance estimated as approximately $1 \times 10^{-4}\,\Omega\,\mathrm{cm}^2$. The device exhibited lasing with clearly observed threshold on the light-current dependence with threshold current density 1.4 kA/cm^2 at 78 K (Fig. 8). Typical spectra of the GaInNAs/GaAs QWs injection microdisk lasers obtained in the temperature range 78–170 K

at $I \sim 1.5 I_{th}$ are shown at Fig. 9. The spectra are multimode in contrast to the case of small-sized optically pumped microdisks. The spectral position of the lasing wavelength does not follow band gap shrinkage and moves faster towards longer wavelength. At 78 K, the lasing wavelength is near the position of the PL maximum of the as-grown structure, while at 170 K, the lasing wavelength is at the long-wavelength part of the spectrum. This can be attributed to the self-heating of the lasers during the current injection. The highest obtained temperature for lasing was 170 K. The threshold current increases approximately by a factor of 5 up to 55 mA in the 77–170 K interval (the inset in Fig. 9). The temperature dependence of the threshold current can be described by exponentially fitting the experimental points with a characteristic temperature $T_0 = 60$ K.

IV. CONCLUSIONS

In summary, optically pumped GaInNAs(Sb)/GaAs(N) quantum well microdisk lasers were studied. The lasing at 1173 nm wavelength with a low threshold (170 μW) was achieved in 3 μm in diameter microdisk with triple GaInNA/
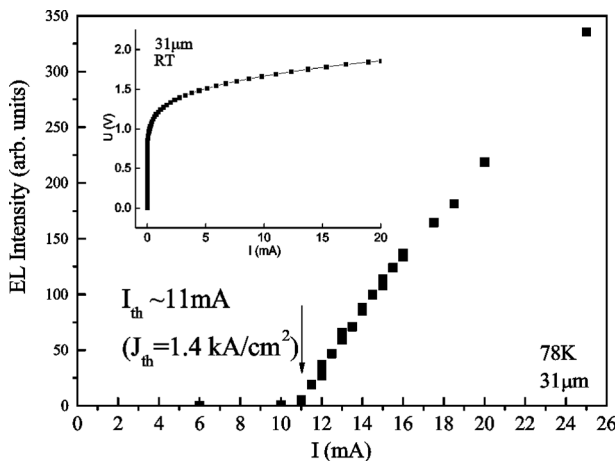

FIG. 8. Light-current curve taken for a D = 31 μm microdisk at 78 K ($\lambda = 1146$ nm). Inset: current-voltage curve at RT.
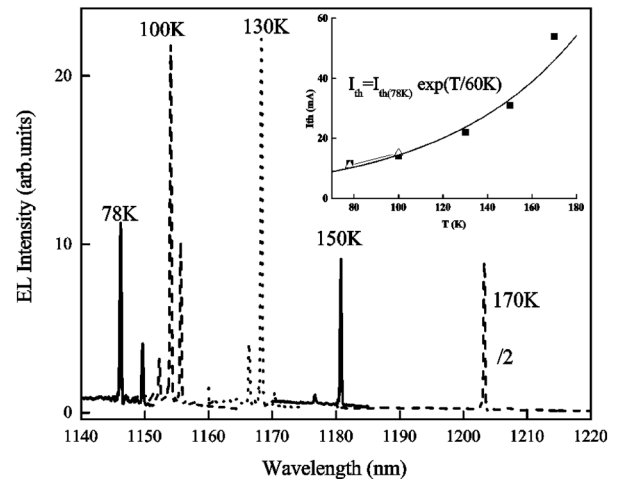

FIG. 9. Typical spectra of the GaInNAs/GaAs QWs injection microdisk laser obtained in temperature range 78–170 K at $I \sim 1.5 I_{th}$. Inset: Temperature dependence of the threshold current.

GaAs QW at 78 K. The use of active region based on single GaInNAsSb QW results in the reduction of the lasing thresholds of the microlasers (within the range of diameters studied in the work) due to the lower density of states. Also, better carrier confinement in GaInNAsSb QW results in higher operation temperature (up to 220 K) before passivation. Sulfur passivation was developed and room temperature single-mode lasing in optically pumped GaInNAs(Sb)/GaAs(N) QW microdisk lasers was demonstrated. Also, the injection 31 μm in diameter microdisk lasers based on GaInNAs/GaAs QW active region were developed and studied. The lasing was observed up to 170 K with a characteristic temperature $T_0 = 60$ K. Evidently, a further improvement in the laser performance is related with the surface passivation process. These results open the way to the development of GaInNAs(Sb)-based ultra-small disk lasers capable to operate at elevated temperatures.

ACKNOWLEDGMENTS

[1] S. Koseki *et al.*, Appl. Phys. Lett. **94**, 051110 (2009).

[2] K. Srinivasan *et al.*, Opt. Express **14**(3), 1094 (2006).

[3] N. V. Kryzhanovskaya, E. I. Moiseev, Yu. V. Kudashova, F. I. Zubov, A. A. Lipovskii, M. M. Kulagina, S. I. Troshkov, Yu. M. Zadiranov, D. A. Livshits, M. V. Maximov, and A. E. Zhukov, Electron. Lett. **51**, 1354 (2015).

[4] C. Gilfert, V. Ivanov, N. Oehl, M. Yacob, and J. P. Reithmaier, Appl. Phys. Lett. **98**, 201102 (2011).

[5] M. V. Maximov, V. M. Ustinov, A. E. Zhukov, N. V. Kryzhanovskaya, A. S. Payusov, I. I. Novikov, N. Y. Gordeev, Y. M. Shernyakov, I. Krestnikov, D. Livshits, S. Mikhrin, and A. Kovsh, Semicond. Sci. Technol. **23**, 105004 (2008).

[6] A. E. Zhukov, N. V. Kryzhanovskaya, M. V. Maximov, A. A. Lipovskii, A. V. Savelyev, A. A. Bogdanov, I. I. Shostak, E. I. Moiseev, D. V. Karpov, J. Laukkanen, and J. Tommila, Semiconductors **48**, 1626 (2014).

[7] M. Fujita, R. Ushigome, and T. Baba, Electron. Lett. **36**, 790 (2000).

[8] D. Liang, M. Fiorentino, S. Srinivasan, J. E. Bowers, and R. G. Beausoleil, IEEE J. Sel. Top. Quantum Electron. **17**, 1528 (2011).

[9] M. Guina and S. H. Wang, "MBE of dilute nitride optoelectronic devices," in *Molecular Beam Epitaxy*, edited by M. Henini (Elsevier, 2013).

[10] T. Takeuchi, Y. L. Chang, A. Tandon, D. Bour, S. Corzine, R. Twist, M. Tan, and H. C. Luan, Appl. Phys. Lett. **80**, 2445 (2002).

[11] N. Tansu, N. J. Kirsch, and L. J. Mawst, Appl. Phys. Lett. **81**, 2523 (2002).

[12] M. Guina, V.-M. Korpijärvi, J. Rautiainen, P. Tuomisto, J. Puustinen, A. Härönen, and O. Okhotnikov, Proc. SPIE **6997**, 69970Q (2008).

[13] S. R. Bank, M. A. Wistey, L. L. Goddard, H. B. Yuen, V. Lordi, and J. S. Harris, IEEE J. Quantum Electron. **40**, 656 (2004).

[14] V.-M. Korpijärvi, E. L. Kantola, T. Leinonen, R. Isoaho, and M. Guina, IEEE J. Sel. Top. Quantum Electron. **21**, 480 (2015).

[15] J. Massies and N. Grandjean, Phys. Rev. B **48**, 8502 (1993).

[16] N. Laurand, S. Calvez, H. D. Sun, M. D. Dawson, J. Gupta, and G. C. Aers, Electron. Lett. **42**, 29 (2006).

[17] M. V. Maximov, N. V. Kryzhanovskaya, A. M. Nadtochiy, E. I. Moiseev, I. I. Shostak, A. A. Bogdanov, Z. F. Sadrieva, A. E. Zhukov, A. A. Lipovskii, D. V. Karpov, J. Laukkanen, and J. Tommila, Nanoscale Res. Lett. **9**, 657 (2014).

[18] N. V. Kryzhanovskaya, M. V. Lebedev, T. V. L'vova, Yu. V. Kudashova, I. I. Shostak, E. I. Moiseev, A. E. Zhukov, M. V. Maximov, M. M. Kulagina, A. M. Nadtochiy, S. I. Troshkov, A. A. Blokhin, and M. A. Bobrov, Tech. Phys. Lett. **41**, 654 (2015).

[19] Y. Yamamoto, S. Machida, and G. Bjork, Phys. Rev. A **44**, 657–668 (1991).

[20] P. Jaffrennou, J. Claudon, M. Bazin, N. S. Malik, S. Reitzenstein, L. Worschech, M. Kamp, A. Forchel, and J.-M. Gerard, Appl. Phys. Lett. **96**, 071103 (2010).

[21] M. K. Chin, D. Y. Chu, and S.-T. Ho, J. Appl. Phys. **75**, 3302 (1994).